

Noncollinear magnetism, spin frustration, and magnetic nanodomains in small Mn_n clusters

José Mejía-López,¹ Aldo H. Romero,² Martin E. Garcia,^{3,*} and J. L. Morán-López⁴

¹*Facultad de Física, Pontificia Universidad Católica de Chile, casilla 306, Santiago 22, Chile*

²*CINVESTAV Querétaro, Libramiento Norponiente No. 2000, 76230 Querétaro, Mexico*

³*Theoretische Physik, Fachbereich Naturwissenschaften, and Center for Interdisciplinary Nanostructure Science and Technology (CINSA), Universität Kassel, Heinrich-Plett-Strasse 40, 34132 Kassel, Germany*

⁴*Advanced Materials Department, IPICYT, Camino Presa San José 2055, 78216, San Luis Potosí, San Luis Potosí, Mexico*

(Received 13 June 2006; revised manuscript received 28 September 2006; published 25 October 2006)

We propose a theoretical explanation for the puzzling size dependence of the magnetic properties of Mn_n clusters. Our approach combines noncollinear *ab initio* calculations and effective spin Hamiltonians. We show that a remarkable interplay between different magnetic couplings, which is already present in the dimer, leads to a complex size-dependent magnetic behavior, dominated by noncollinear magnetism, frustration, and small cluster magnetic moments. Our results are in good agreement with experiment.

DOI: [10.1103/PhysRevB.74.140405](https://doi.org/10.1103/PhysRevB.74.140405)

PACS number(s): 75.75.+a, 36.40.Cg, 31.15.Ar

The evolution of magnetism from the atom to the bulk constitutes a fundamental problem of basic and applied physics, and its correct description is indispensable for the understanding of magnetism at the nanoscale. Recently, a particularly exotic behavior of the magnetic moments as a function of size was experimentally found for Mn_n clusters,^{1,2} which poses a challenging problem. Here, we present a theoretical description of these findings.

Manganese is a unique element which exhibits a variety of unusual electronic and magnetic properties depending on the environment.³⁻¹⁰ For instance, the bulk-crystal structure of α -Mn is remarkably complex. It contains 29 atoms in the unit cell and shows antiferromagnetic ordering. On the other hand, dilute solutions of Mn in Cu behave like spin glasses.³ Also the compounds known as manganites show fascinating magnetic properties.⁴ In addition, Mn_{12} complexes act as molecular magnets, exhibiting resonant tunneling between spin states⁵ and forming “nanodomains.”⁶⁻⁸ Finally, the manganese dimer is partially van der Waals bonded and also seems to exhibit antiferromagnetic behavior.⁹⁻¹¹

Consistently with the remarkable properties of Mn compounds mentioned above, and despite the similar magnetic ordering of Mn_2 and Mn bulk, experiments show that small manganese clusters exhibit an intriguing magnetic behavior, with signatures of superparamagnetism and magnetic moments $\mu(n)$ smaller than $1.5\mu_B$ per atom.^{1,2,8,9,13} When manganese magnetic clusters are deposited on a metallic surface, they can magnetically couple to very long range, mediated by the surface metallic electrons.¹⁴ As the cluster size increases, the behavior of $\mu(n)$ as a function of n is strongly nonmonotonic.^{1,2}

In recent years, different theoretical determinations of the magnetic and electronic structure of Mn_n clusters have been reported.^{12,15-17} Almost all calculations have in common the assumption of collinear spins, but give contradictory results. A careful analysis within an all-electron scheme came to the conclusion that Mn_2 exhibits multiple magnetic and structural minima.¹⁵

The experimental evidence and the theoretical works mentioned above suggest that the most probable scenario for small Mn clusters is that of almost degenerate different spin configurations. Therefore, the correct approach to describe

their magnetic structure must give up the assumption of collinearity. This was confirmed recently by a calculation which yields a noncollinear magnetic configuration for Mn_6 .¹⁷ Moreover, the fact that the ferromagnetic and antiferromagnetic solutions are very close in energy, in particular for very small clusters,¹⁶ could also lead to spin frustration in larger clusters. This effect has not been theoretically analyzed so far. Moreover, the overall size dependence of $\mu(n)$ measured by Knickelbein^{1,2} remains unexplained. In this Rapid Communication, we present the first theoretical description of the size dependence $\mu(n)$ for Mn_n clusters up to $n=40$, which accounts for most of the experimental findings.

We performed first a noncollinear *ab initio* determination of the magnetic properties of small Mn_n clusters in the range $2 \leq n \leq 8$. Our results suggest that in small Mn_n clusters a remarkable competition between kinetic and exchange-correlation energies leads to almost degenerate spin configurations, which results in the formation of noncollinear magnetic nanodomains in order to avoid spin frustration. Moreover, with the help of the data obtained from the *ab initio* calculations we fit the parameters of an effective spin Hamiltonian, which we use to calculate $\mu(n)$ for larger clusters ($9 \leq n \leq 40$). This model gives very good agreement with the puzzling experimental results.

To determine the electronic and magnetic properties of the clusters in the range $2 \leq n \leq 8$ we have used the SIESTA code,¹⁸ which performs a fully self-consistent density-functional calculation to solve the Kohn-Sham equations. We included spin polarization, both collinear and noncollinear,¹⁹ in the local-density approximation (LDA). The ionic pseudopotentials²⁰ were generated from the atomic configurations $[Ne]3s^23p^63d^5$, core radii 1.50, 1.50, 1.30, and 2.20 a.u. for the s , p , d , and f components, respectively, and a core correction of 0.7 a.u. The basis set used for the present work to describe the valence states is a double- ζ set with a confining energy shift of 50 meV.

The calculations have been performed in the following way. First, clusters were completely relaxed with respect to their ionic and electronic degrees of freedom, assuming a given magnetic configuration (ferro- or antiferromagnetic), and different structural geometries. Once the ground-state geometry was obtained, we included the spin orientation of

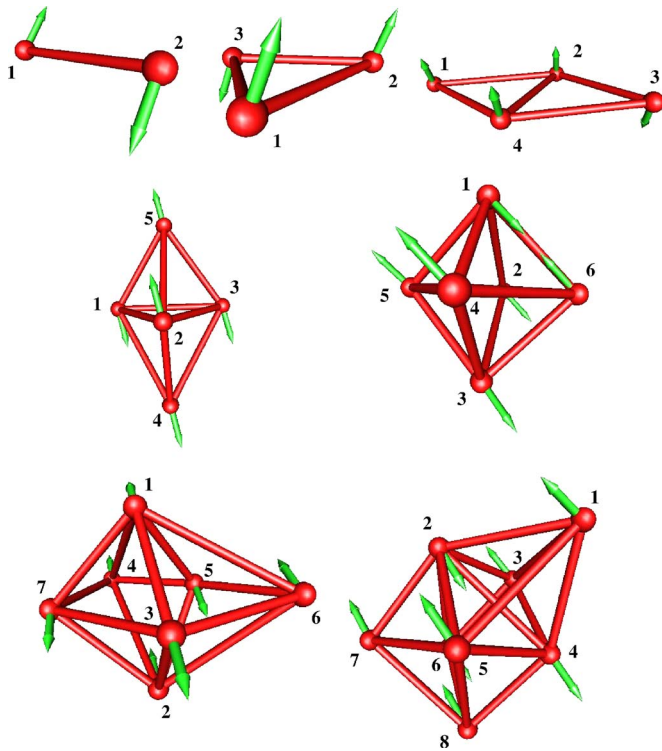


FIG. 1. (Color online) Ground-state structures of Mn_n clusters, for $n=2-8$, optimized with respect to the electronic, ionic, and spin degrees of freedom. The magnitude and orientation of the quantum expectation value of the spin at each atom are indicated by arrows.

the individual atoms as additional degrees of freedom and minimized again the whole set of variables. Different calculations with different initial spin configurations have been performed to avoid trapping into local energy minima.

In Fig. 1 we show the ground-state structures and spin configurations obtained from the *ab initio* calculations. Interestingly, most of these clusters, in particular $n=6, 7$, and 8 , show noncollinear magnetic behavior. This indicates that previous theoretical studies, with the exception of Ref. 17, missed an essential ingredient for the correct physical description of these systems. As can be seen from Fig. 1, some of the clusters show a marked Jahn-Teller distortion, like Mn_3 and Mn_4 . As a general rule, the average magnetic moment μ of these clusters is at least two times smaller than the moment of an isolated Mn atom. The average magnetic moments obtained are $\mu(2)=0$, $\mu(3)=1.67\mu_B$, $\mu(4)=2.5\mu_B$, $\mu(5)=1.0\mu_B$, $\mu(6)=0.87\mu_B$, $\mu(7)=0.99\mu_B$, and $\mu(8)=1.17\mu_B$. Note that the lowest energy structure of Mn_5 corresponds to an almost bipyramidal configuration. However, symmetry is broken due to the formation of domains. A similar effect is present for $n=6, 7$, and 8 . Apart from the noncollinear behavior, the most important feature of the magnetic configurations shown in Fig. 1 is that manganese atoms separated by short distances are mostly coupled antiferromagnetically, whereas for long interatomic distances the coupling is mostly ferromagnetic. This remarkable effect leads to spin frustration and to the formation of noncollinear nanodomains, i.e., as clearly shown in Fig. 1. We call nanodomains to subgroups of neighboring atoms aligned ferromagnetically to each other.

TABLE I. Energy differences (in meV) of the collinear and noncollinear magnetic configurations of Mn_n clusters with respect to the structure with the lowest energy.

| | Mn_2 | Mn_3 | Mn_4 | Mn_5 | Mn_6 | Mn_7 | Mn_8 |
|-----------------|--------|--------|--------|--------|--------|--------|--------|
| ΔE_{AF} | 0 | 16 | 21 | 1 | 85.5 | 118 | 43 |
| ΔE_{FM} | 10 | 46 | 21 | 505 | 564 | 1624 | 43 |
| ΔE_{NC} | 0 | 0 | 0 | 0 | 0 | 0 | 0 |

To understand the origin of the noncollinearity and quantify its strength, we have also calculated the cohesive energies of the ferromagnetic and antiferromagnetic configurations in the ground-state geometries, assuming collinear arrangements. In Table I we show the energy differences between the noncollinear ground states and the energies obtained assuming collinear spins for the same geometries. Note that for all sizes considered, the energy difference between the noncollinear and the collinear arrangements is very small. This is consistent with the multiplicity of minima obtained in previous collinear theoretical studies.¹⁵ Furthermore, the energy differences $\Delta E = E_{AF} - E_{FM}$ between the antiferromagnetic (AF) and the ferromagnetic (FM) configurations is also very small. The origin of this behavior is that the different terms involved in ΔE , from whose competition the magnetic behavior arises, almost cancel themselves in Mn, as we discuss below in detail.

In fact, the nature of magnetism in small Mn_n clusters can be inferred from the magnetic behavior in the dimer. Although almost all *ab initio* studies performed so far for Mn_2 obtained a ferromagnetic configuration, our calculations yield an antiferromagnetic state, with a bond length of $r_0 = 2.890 \text{ \AA}$ (binding energy of 0.391 eV). This result for the magnetic ordering of the dimer is in agreement with the existing experimental evidences.^{9,10} However, it must be pointed out that the ferromagnetic, antiferromagnetic and noncollinear states are almost degenerate (see Table I). In our calculations the interatomic distance is underestimated, as in other works based on the LDA.^{15,17} Interestingly, if we now force the interatomic distance to be equal to the experimental value $r_0^{exp} = 3.18 \text{ \AA}$,¹³ we obtain a ferromagnetic ground state. This fact originates from the remarkable distance dependence exhibited by the magnetic coupling. To analyze this in detail we plot in Fig. 2 the total energy of the dimer as a function of the bond length d for the collinear ferromagnetic and antiferromagnetic configurations and also for the noncollinear solution. The most important feature of Fig. 2 is that there is a crossing between the FM and AF curves at $d_c = 3.06 \text{ \AA}$, which determines the interatomic distance at which the ground state changes from anti- to ferromagnetic. Note that the energy of the noncollinear solution coincides with the AF curve for distances for $d < d_c$ and with the FM curve for $d > d_c$. This means that the dimer shows collinear magnetism for almost all distances. However, we obtain an interesting behavior around $d = d_c$, where the noncollinear solution has a slightly lower energy than the collinear curves. This is due to the fact that at this point the AF and FM states have the same energy and therefore an intermediate noncollinear state leads to an energy decrease.

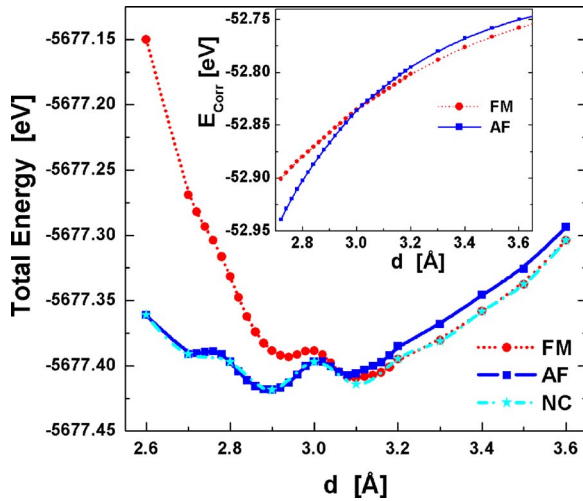


FIG. 2. (Color online) Total electronic energy of Mn_2 as a function of the interatomic distance for the noncollinear, ferromagnetic, and antiferromagnetic cases. The crossing at $d=3.06$ Å can be clearly observed. Inset: distance dependence of the correlation energy for Mn_2 as function of distance for the ferro- and antiferromagnetic configurations. Note that the crossing occurs at the same distance as for the total energies.

Another important feature shown by Fig. 2 is the appearance of many minima in all three energy curves. They are due to presence of competing interactions. The different energy terms (exchange, correlation, kinetic energy, Hartree energy, and core-core repulsion) compensate each other in such a way that small variations in magnitude of these terms lead to shifts, amplification, or disappearance of some of the minima.²¹ Notice that inclusion of van der Waals interactions (which are not taken into account by the LDA and its corrections) might lead to a change of the depths of the different minima.

It is important to point out that the Mn dimer is believed to be partially bonded by electronic effects and partially by van der Waals interactions.¹¹ These last interactions cannot be well described by the LDA and its corrections. Thus, our calculations for Mn_2 are not aimed at correctly describing the nature of the bonding of the real dimer, but at taking it as a model for a bonding between two Mn atoms in Mn_n .

We have compared the distance dependence of the different terms contributing to the cohesive energy of the dimer. It turns out that most of the energies cancel each other, so that the correlation energy plays a fundamental role. In the inset of Fig. 2 we show the bond-length dependence of the correlation energy for the ferromagnetic and antiferromagnetic configurations. Notice that for $d < d_c$ the correlation energy favors antiferromagnetic behavior, while for larger distances the correlation energy term of the ferromagnetic state becomes slightly more important. Remarkably, both terms are of comparable size over a broad range of distances, which results in a delicate energy balance and the possibility of instabilities, degenerate states, and multiple minima. Since the FM and the AF configurations of the dimer are very close in energy, and due to the change of magnetic character for increasing distances, one should not expect a clear magnetic ordering in small clusters, but rather a competition between

both types. The fact that nearest neighbors will tend to order antiferromagnetically, whereas further neighbors will favor a ferromagnetic ordering leads to noncollinear effects, domain formation, in order to avoid spin frustration as much as possible.

The behavior shown in Fig. 2 can be interpreted as follows. For short interatomic distances the strong overlap of $3d$ orbitals leads to electron delocalization, which favors antiferromagnetism. In contrast, for long distances, localization becomes more important and ferromagnetic correlations dominate. This explains the calculated spin configurations for Mn_5 to Mn_8 (Fig. 1).

One can interpret the crossing of energy curves in the framework of magnetic coupling constants. We have determined the effective exchange coupling constant $J(d)$ between localized spins at the Mn atoms as $J(d) = [E(d)^{\uparrow\downarrow} - E(d)^{\uparrow\uparrow}] / 0.5$ as a function of the interatomic distance d . Obviously, we obtain $J > 0$ for $d < d_c$ (antiferromagnetic coupling) and $J < 0$ for $d > d_c$ (ferromagnetic coupling). Now, and in order to determine the magnetic properties of clusters with n up to 40, which cannot be done yet using *ab initio* approaches, we propose an effective spin Hamiltonian of the form

$$H = \sum_{\substack{i,j=1,n \\ i \neq j}}^n J_{ij} \vec{S}_i \cdot \vec{S}_j + V(\{|\vec{r}_i - \vec{r}_j|\}), \quad (1)$$

where the \vec{S}_i are classical spins, with magnitudes measured in Bohr magnetons. The exchange coupling constants J_{ij} are the distance-dependent quantities $J(|\vec{r}_i - \vec{r}_j|)$, $|\vec{r}_i - \vec{r}_j|$ being the distance between atoms i and j . We use for $J(|\vec{r}_i - \vec{r}_j|)$ the function $J(d)$ extracted from the dimer. Moreover, we analyzed carefully the local magnetic moments S_i obtained from the *ab initio* calculations (Mn_2 to Mn_8) as a function of the coordination number z , and we obtained a clear relation between them. It turns out that a function of the form $S = 4.42 - 0.5z$ for $z \leq 8$ and $S_i = 0.4$ for $z > 8$ reproduces the results obtained for small clusters. The coordination number z_i of atom i is defined as the number of neighbors being at a distance smaller than 2.26 Å (nearest-neighbor distance in bulk Mn) from atom i . It must be pointed out that, although the spins \vec{S}_i are treated as classical, the scalar product is taken into account. Therefore, the Hamiltonian H intrinsically includes noncollinearity. Note that the approximation of classical spins is justified by the high local moments of Mn, and is also used for the description of manganites.⁴ In Eq. (1), $V(\{|\vec{r}_i - \vec{r}_j|\})$ is, in general, a many-body potential which models the cohesive energy of the cluster. For simplicity, we take a Lennard-Jones-type (LJ) potential in order to generate compact structures, which are expected for clusters in the size range we are interested in. Since we seek for a qualitative explanation of the size dependence of the magnetic properties of these clusters, a simple LJ potential should work reasonably well for our purposes. We minimized H numerically, by using genetic algorithms (a more detailed description for a different system is discussed in Ref. 22), and obtained the ground-state spin configurations for clusters

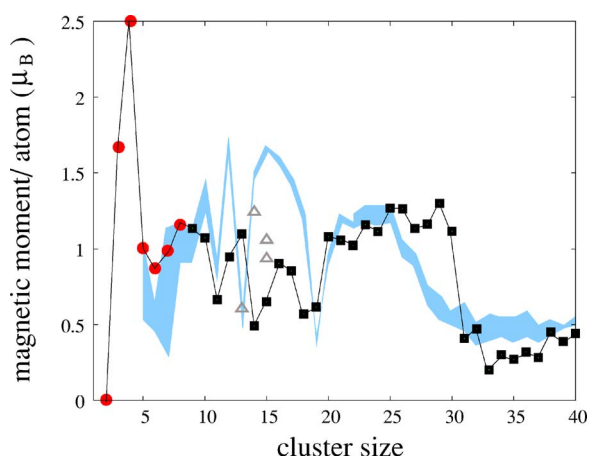


FIG. 3. (Color online) Size dependence of the magnetic moment per atom μ (in units of μ_B) of Mn_n clusters in the size range $2 \leq n \leq 40$. Red (dark gray) circles correspond to the *ab initio* results. Squares show the calculated μ for compact structures using the classical spin Hamiltonian of Eq. (1). Gray open triangles refer to isomers having smaller cohesive energies. The light blue (light gray) shadowed zone corresponds to the experimental results of Refs. 1 and 2 taken into account the reported error bars.

up to Mn_{40} . The calculated size dependence of the magnetic moments per atom is shown in Fig. 3, where we also show the *ab initio* results. Clearly, the orders of magnitude of the all calculated magnetic moments are in good agreement with experiment. Moreover, the overall size dependence $\mu(n)$ is well described and shows a complex behavior, as in the experiment.^{1,2} Note that in our results the oscillations as a function of n between $n=6$ and $n=13$, $n=14$ and $n=20$, and between $n=21$ and $n=31$, observed in experiment, are very well reproduced.

In Fig. 3 we also show the magnetic moments of isomers of Mn_{13} , Mn_{14} , and Mn_{15} which have smaller cohesive energy than the ground-state structures, but which might also be present in the cluster beam on which experiments have been performed. The good agreement between our model

and experiment indicates that the physics underlying our model is correct, i.e., the magnetic properties of Mn_n clusters are dominated by spin frustration due to the presence of different spin-spin coupling constants, which leads to noncollinear magnetism and formation of nanodomains. As a consequence, $\mu(n)$ shows a complex form and low magnetic moments, which reflect the least frustrated possible spin configurations.

Finally, we mention that we have tested our approach and our results by performing calculations using other pseudopotentials and basis sets, other implementations of density functional theory (plane waves), and other functionals [the generalized gradient approximation (GGA)]. No changes to the physical picture and to the conclusions of this work were obtained.²³

Summarizing, we presented an explanation for the puzzling behavior of $\mu(n)$ for Mn_n clusters up to $n=40$. Note that the experimentally obtained $\mu(n)$ shows a further oscillation between $n \sim 40$ and $n \sim 80$. We believe that this feature is due to the interplay between structure and magnetism. For those sizes, the cluster structure tends to acquire some signatures of α -Mn. On the other hand, the ferromagnetic coupling is still present. Thus, a competition between cohesion and magnetic energy takes place. Between $n \sim 40$ and $n \sim 80$ the magnetic energy seems to dominate. According to this idea, for clusters with $n > 80$ the structures should slowly converge to the bulk one and the magnetic ordering approach the antiferromagnetic state of α -Mn. In order to describe such a competition, a more accurate description of $V(\{\vec{r}_i, -\vec{r}_j\})$ is needed. Research in this direction is in progress.

J.M. acknowledges support from FONDECYT under Grants No. 1050066 and No. 7050111, and from the Millennium Sciences Nucleus “Condensed Matter Physics” P02-054F. A.H.R. is supported by Project No. J-42647-F from CONACYT-Mexico. M.E.G. acknowledges kind hospitality at the IPICYT and also support from the DFG through the SPP1153.

*Electronic mail: garcia@physik.uni-kassel.de

¹M. B. Knickelbein, Phys. Rev. Lett. **86**, 5255 (2001).

²M. B. Knickelbein, Phys. Rev. B **70**, 014424 (2004).

³D. Chu *et al.*, Phys. Rev. Lett. **72**, 3270 (1994).

⁴Elbio Dagotto, in *The Physics of Manganites and Related Compounds*, Springer Series in Solid-State Sciences Vol. 136 (Springer, Berlin, 2003).

⁵J. R. Friedman *et al.*, Phys. Rev. Lett. **76**, 3830 (1996).

⁶W. Wensdorfer *et al.*, Nature (London) **416**, 406 (2002).

⁷R. Sessoli *et al.*, Nature (London) **365**, 141 (1993).

⁸K. M. Mertens *et al.*, Solid State Commun. **127**, 131 (2003).

⁹C. A. Baumann *et al.*, J. Chem. Phys. **78**, 190 (1983).

¹⁰J. R. Lombardi and B. Davids, Chem. Rev. (Washington, D.C.) **102**, 2431 (2002).

¹¹S. Yamamoto *et al.*, J. Chem. Phys. **124**, 124302 (2006).

¹²T. M. Briere *et al.*, Phys. Rev. B **66**, 064412 (2002).

¹³R. J. Van Zee *et al.*, J. Chem. Phys. **76**, 5636 (1982).

¹⁴V. S. Stepanyuk *et al.*, Phys. Rev. B **70**, 075414 (2004).

¹⁵M. R. Pederson *et al.*, Phys. Rev. B **58**, 5632 (1998).

¹⁶P. Bobadova-Parvanova *et al.*, Phys. Rev. A **67**, 061202(R) (2003); J. Chem. Phys. **122**, 014310 (2005).

¹⁷T. Morisato *et al.*, Phys. Rev. B **72**, 014435 (2005); R. C. Longo *et al.*, *ibid.* **72**, 174409 (2005).

¹⁸E. Artacho *et al.*, Phys. Status Solidi B **215**, 809 (1999).

¹⁹T. Oda *et al.*, Phys. Rev. Lett. **80**, 3622 (1998).

²⁰N. Troullier and J. L. Martins, Phys. Rev. B **43**, 1993 (1991).

²¹The depths of all energy minima of Fig. 2 are larger than the error $\Delta\epsilon$ of the energy calculations. $\Delta\epsilon < 1$ meV, whereas the heights of the energy barriers are at least 5 meV.

²²A. H. Romero and J. Mejía-López, Physica B **384**, 244 (2006).

²³The GGA calculations for Mn_2 yield $r_0=3.02$ Å (AF) and $d_c=3.10$ Å.